Short Papers

Electromagnetic Analysis of Spherical Dielectric Shielded Resonators

ANNE JULIEN AND PIERRE GUILLON

Abstract—**We present in this paper, the electromagnetic parameters of free and shielded dielectric spherical resonators for their utilization in the millimeter-wave frequency band.**

I. Introduction

For many years, dielectric resonators have been of considerable interest in microwave techniques. They are used in a number of different applications at high frequencies (filters, oscillators, etc.)

We have studied dielectric resonator behavior for millimeter-wave frequencies (through 90 GHz). In this case, the dimensions of dielectric samples are very small, so, we will use spherical dielectric resonators that are easier to produce than the cylindrical ones. This type of shielded dielectric resonator could be inserted into microstrip, fin lines or waveguide structures to realize passive circuits (bandstop and bandpass filters) which in turn could be coupled with active circuits to stabilize the resonant frequency of an oscillator.

Several publications about dielectric spheres have been presented [1]–[7].

The present work analyzes the electromagnetic parameters of free and shielded dielectric spheres. In each case, the frequencies and the Q factor are calculated.

II. Free Dielectric Sphere

A. Fields Expressions

Let us consider a dielectric spherical sample (permittivity ϵ_r and radius a) placed in an infinite, linear, homogeneous, and isotropic medium (Fig 1). The electromagnetic fields existing in the system satisfy Maxwell's equations. It's possible to class the waves as transverse electric modes (TE) and transverse magnetic modes (TM).

After expansion and simplification of Maxwell's equations in a spherical coordinates system (r, θ, ϕ) we obtain the spherical wave equation

$$\frac{\partial^2\psi}{\partial r^2}+\frac{2}{r}\frac{\partial\psi}{\partial r}+\frac{1}{r^2\sin\theta}\frac{\partial}{\partial\theta}\left(\sin\theta\frac{\partial\psi}{\partial\theta}\right)+\frac{1}{r^2\sin^2\theta}\frac{\partial^2\psi}{\partial\phi^2}+\omega^2\epsilon\mu_0\psi=0 \quad (1)$$

where ψ is a function of r, θ, and ϕ.

Manuscript received July 2, 1985; revised December 4, 1985. This work was supported in part by the French Ministère de la Recherche Scientifique.

The authors are with Laboratoire de Communications Optiques et Micro-ondes, Laboratoire Associe au C.N.R.S., F-87060 Limoges Cedex, France.

IEEE Log Number 8607970.

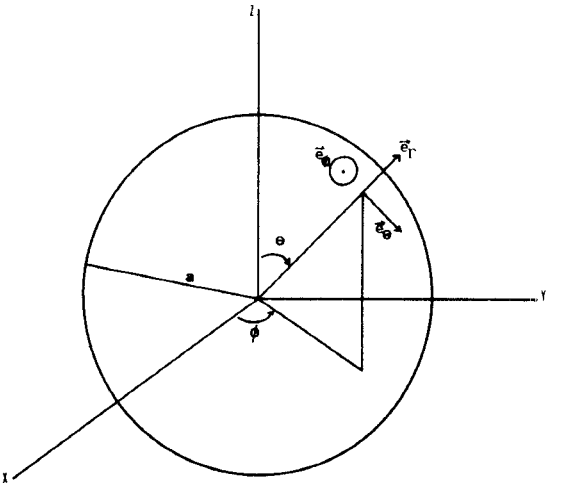

Fig. 1. Spherical dielectric resonator.

The solution is found by applying the separating variable method

$$\psi = f(r)\cdot g(\theta)\cdot h(\phi). \quad (2)$$

According to $r \leqslant a$ or $r \geqslant a$, we obtain the fields' expressions given in the following form:

$$\mathrm{TE}_{nml} \text{ mode}$$

where n corresponds to the variation of r, m corresponds to the variation of ϕ, l defines the lth root of the characteristic equation (5a).

For $r \leqslant a$

$$E_r = 0$$

$$E_\theta = \frac{-j\omega\mu_0}{\sqrt{kr}\sin\theta} mAJ_{n+1/2}(kr)\,P_n^m(\cos\theta)\begin{matrix}-\sin\\\cos\end{matrix} m\phi$$

$$E_\phi = \frac{j\omega\mu_0}{\sqrt{kr}} AJ_{n+1/2}(kr)\frac{d}{d\theta}\left(P_n^m(\cos\theta)\right)\begin{matrix}\cos\\\sin\end{matrix} m\phi$$

$$H_r = \frac{n(n+1)}{r^{3/2}}\frac{A}{\sqrt{k}}J_{n+1/2}(kr)\,P_n^m(\cos\theta)\begin{matrix}\cos\\\sin\end{matrix} m\phi$$

$$H_\theta = \frac{A}{r\sqrt{k}}\frac{d}{dr}\left(\sqrt{r}J_{n+1/2}(kr)\right)\frac{d}{d\theta}\left(P_n^m(\cos\theta)\right)\begin{matrix}\cos\\\sin\end{matrix} m\phi$$

$$H_\phi = \frac{mA}{\sin\theta\sqrt{k}\,r}\frac{d}{dr}\left(\sqrt{r}J_{n+1/2}(kr)\right)P_n^m(\cos\theta)\begin{matrix}-\sin\\\cos\end{matrix} m\phi. \quad (3)$$

We have chosen the solution $J_{n+1/2}(kr)$ (the first Bessel function of $n+\frac{1}{2}$ order in kr with $k=\omega\sqrt{\epsilon_r}/c$) taking into account that the energy inside the sphere must be finite. $P_n^m(\cos\theta)$ is the first kind associated Legendre function of orders n, m, in $\cos\theta$. A is a constant.

0018-9480/86/0600-0723$01.00 ©1986 IEEE

For $r \geq a$

$$E_r = 0$$

$$E_\theta = \frac{-j\omega\mu_0}{\sqrt{k_0 r}\sin\theta} mBH^{(2)}_{n+1/2}(k_0 r) \cdot P_n^m(\cos\theta) \begin{matrix}-\sin\\ \cos\end{matrix} m\phi$$

$$E_\phi = \frac{j\omega\mu_0}{\sqrt{k_0 r}} BH^{(2)}_{n+1/2}(k_0 r)\frac{d}{d\theta}(P_n^m(\cos\theta)) \begin{matrix}\cos\\ \sin\end{matrix} m\phi$$

$$H_r = \frac{n(n+1)}{r^{3/2}}\frac{B}{\sqrt{k_0}} H^{(2)}_{n+1/2}(k_0 r) P_n^m(\cos\theta) \begin{matrix}\cos\\ \sin\end{matrix} m\phi$$

$$H_\theta = \frac{B}{\sqrt{k_0 r}}\frac{d}{dr}\left(\sqrt{r} H^{(2)}_{n+1/2}(k_0 r)\right)\frac{d}{d\theta} \cdot (P_n^m(\cos\theta)) \begin{matrix}\cos\\ \sin\end{matrix} m\phi$$

$$H_\phi = \frac{mB}{r\sin\theta\sqrt{k_0}}\frac{d}{dr}\left(\sqrt{r} H^{(2)}_{n+1/2}(k_0 r)\right) \cdot P_n^m(\cos\theta) \begin{matrix}-\sin\\ \cos\end{matrix} m\phi. \quad (4)$$

We have chosen the solution $H^{(2)}_{n+1/2}(k_0 r)$, the Hankel function of the second kind of the order $n+\frac{1}{2}$ in $k_0 r$, with $k_0 = \omega/c$ having zero energy at infinity

$$\mathrm{TM}_{nml}\ \text{Mode.}$$

For TM_{nml} modes, the fields' expressions are of the same type, but we may introduce the characteristic impedance that depends on the permittivity $\epsilon(=\epsilon_0\epsilon_r)$ of the media that we consider.

B. Characteristic Equation

To establish the resonant condition of the inhomogeneous dielectric system, we write the continuity condition in $r = a$. So we obtain a characteristic equation available, respectively, for TE_{nml} and TM_{nml} modes

$$\frac{J_{n-1/2}(ka)}{J_{n+1/2}(ka)} = \frac{1}{\sqrt{\epsilon_r}}\frac{H^{(2)}_{n-1/2}(k_0 a)}{H^{(2)}_{n+1/2}(k_0 a)} \quad (5a)$$

$$-\frac{n}{ka} + \frac{J_{n-1/2}(ka)}{J_{n+1/2}(ka)} = \frac{-n\sqrt{\epsilon_r}}{k_0 a} + \sqrt{\epsilon_r}\frac{H^{(2)}_{n-1/2}(k_0 a)}{H^{(2)}_{n+1/2}(k_0 a)}. \quad (5b)$$

To solve these equations, we introduce a complex pulsation $\omega = \omega' - j\omega''$, which is the pulsation of free oscillations, taking into account the damp outside the dielectric resonator. The real value ω', introduces the resonant frequency of the free dielectric sphere: $f_0 = \omega'/2\pi$. The imaginary part ω'', corresponds to the radiation losses. The energy in the dielectric sphere can be written as follows:

$$\overline{W}_m(t) = \overline{W}_m(0)\, e^{-2\omega'' t}.$$

Let $\overline{W}_p$ be the radiated energy

$$\overline{W}_p = \frac{-d}{dt}(\overline{W}_m(t)) = 2\omega''\overline{W}_m(t)$$

so $\omega'' = \overline{W}_p/2\overline{W}_m$.

With this assumption, we can define the radiation quality factor Q_r of the free spherical dielectric resonator

$$Q_r = \omega'\overline{W}_m/\overline{W}_p = \omega'/2\omega''.$$

We substitute into (5a) and (5b), respectively, ka and $k_0 a$ by their expressions in (6):

$$ka = \omega a/c = (\omega' - j\omega'')a/c = X - jY$$

$$k_0 a = ka/\sqrt{\epsilon_r} = X' - jY'4$$

with

$$X' = X/\sqrt{\epsilon_r},\quad Y' = Y/\sqrt{\epsilon_r} \quad (6)$$

and we use a computer to find the values of X, X', Y, and Y' satisfying (5a) and (5b).

TABLE I

MODE	RADIUS a(mm)	RESONANT FREQUENCY f_0 (Ghz)
TE_{101}	1.56	15.66
	0.72	33.9
TE_{102}	1.56	33.92
	0.72	73.5
TM_{101}	1.56	22.5
	0.72	48.8
TM_{102}	1.56	35.2
	0.72	76.3

TABLE II

MODE	RADIUS a(mm)	RESONANT FREQUENCY f_0 (Ghz)
TE_{101}	1.56	29.7
	0.72	63.1
TE_{102}	1.56	59.8
	0.72	134

C. Results of Computation

An example of the results that we can obtain is presented in Table I for different modes and dimensions of dielectric samples (of permittivity $\epsilon_r = 36$).

A new material having been produced recently by NTK [8], for which the product $(f_1/tg\delta) = 350\,000$ and the permittivity $\epsilon_r = 9.7$. Some results are given (Table II).

Some radiated Q also have been computed. For example, we found

for TE_{101} mode with $\epsilon_r = 36$ $Q_r = 31.4$
with $\epsilon_r = 9.7$ $Q_r = 8$

for TE_{102} mode with $\epsilon_r = 36$ $Q_r = 27.3$
with $\epsilon_r = 9.7$ $Q_r = 9$.

II. Shielded Dielectric Sphere

A. Fields Expressions

We now suppose that we have the system consisting of: a dielectric sphere (permittivity ϵ_r and radius a), shielded by a spherical metallic cavity of radius b (Fig 2). Such a structure approximates the spherical dielectric resonator inserted into a waveguide if the dimensions of the metallic sphere are near to the inside dimensions of the waveguide.

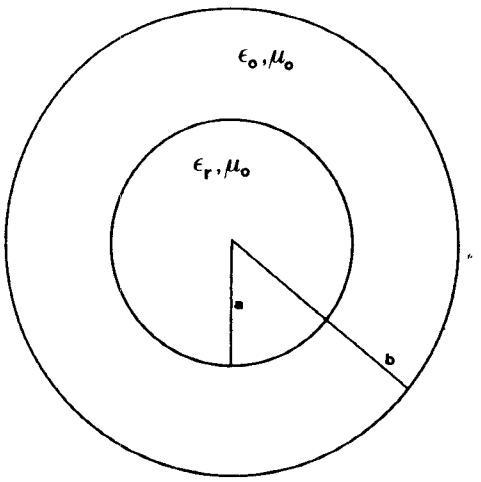

Fig. 2. Shielded dielectric sphere.

Applying Maxwell's equations, we obtain the same wave equation of that used for free spheres. So, for $r \leqslant a$, we preserve the same fields' expressions. For $a \leqslant r \leqslant b$, we choose a solution that is a linear combination of $J_{n+1/2}$ and $Y_{n+1/2}$ (the second kind of Bessel function of the order $n+\frac{1}{2}$ in $k_0 r$ with $k_0 = \omega/c$) and obtain

$$\mathrm{TE}_{nml} \text{ mode}$$

for $a \leqslant r \leqslant b$

$$E_r = 0$$

$$E_\theta = \frac{-j\omega\mu_0}{\sqrt{k_0 r}\sin\theta} m\left(BJ_{n+1/2}(k_0 r) + CY_{n+1/2}(k_0 r)\right) \cdot P_n^m(\cos\theta) \begin{matrix}-\sin \\ \cos\end{matrix} m\phi$$

$$E_\phi = \frac{j\omega\mu_0}{\sqrt{k_0 r}}\left(BJ_{n+1/2}(k_0 r) + CY_{n+1/2}(k_0 r)\right)\frac{d}{d\theta} \cdot \left(P_n^m(\cos\theta)\right) \begin{matrix}\cos \\ \sin\end{matrix} m\phi$$

$$H_r = \frac{n(n+1)}{r^{3/2}k_0}\left(BJ_{n+1/2}(k_0 r) + CY_{n+1/2}(k_0 r)\right) \cdot \left(P_n^m(\cos\theta)\right) \begin{matrix}\cos \\ \sin\end{matrix} m\phi$$

$$H_\theta = \frac{1}{r\sqrt{k_0}}\frac{d}{dr} \cdot \left(\sqrt{r}\left(BJ_{n+1/2}(k_0 r) + CY_{n+1/2}(k_0 r)\right)\right)\frac{d}{d\theta} \cdot \left(P_n^m(\cos\theta)\right) \begin{matrix}\cos \\ \sin\end{matrix} m\phi$$

$$H_\phi = \frac{m}{r\sin\theta\sqrt{k_0}}\frac{d}{dr} \cdot \left(\sqrt{r}\left(BJ_{n+1/2}(k_0 r) + CY_{n+1/2}(k_0 r)\right)\right) \cdot P_n^m(\cos\theta) \begin{matrix}-\sin \\ \cos\end{matrix} m\phi \qquad (7)$$

$$\mathrm{TM}_{nml} \text{ mode}$$

for $a \leqslant r \leqslant b$.

As we did previously, we permute the E and H fields without forgetting $\sqrt{\mu/\epsilon}$.

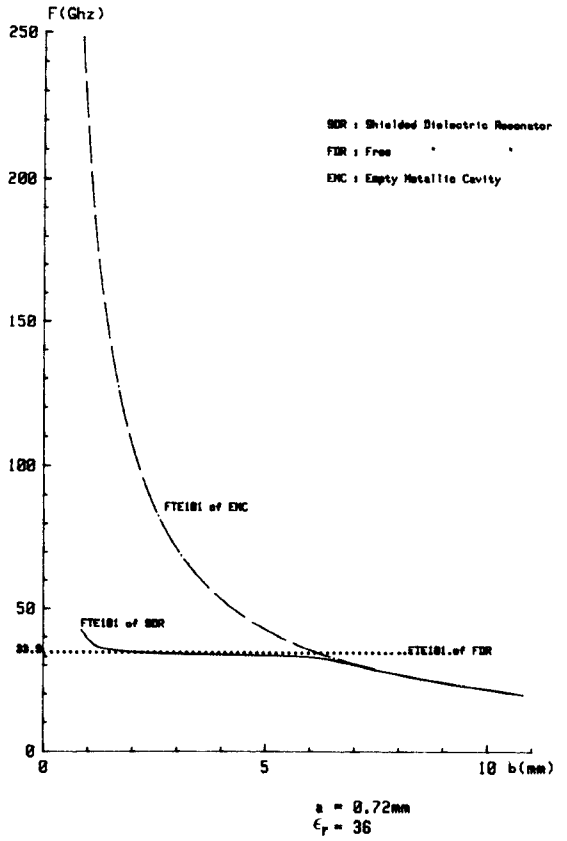

Fig. 3. Resonant frequency variations of the shielded dielectric resonator (SDR) for TE_{101} mode.

B. Characteristic Equations

We satisfy the continuity conditions on the dielectric interfaces at $r = a$ and the boundary conditions on the metallic surface situated at $r = b$

1) Continuity at $r = a$ of the tangential components of E and H fields.

2) Tangential electric field must be zero at $r = b$.

After some manipulations, we obtain, respectively, for TE_{nml} and TM_{nml} modes

$$Y_{n+1/2}(k_0 b)\left\{J_{n+1/2}(ka)J'_{n+1/2}(k_0 a) - \sqrt{\epsilon r}\,J_{n+1/2}(k_0 a)J'_{n+1/2}(ka)\right\} = J_{n+1/2}(k_0 b)\left\{J_{n+1/2}(ka)Y'_{n+1/2}(k_0 a) - \sqrt{\epsilon r}\,Y_{n+1/2}(k_0 a)J'_{n+1/2}(ka)\right\}$$

$$\frac{\epsilon - \epsilon_0}{2a}J_{n+1/2}(ka)\left\{J_{n+1/2}(k_0 a)\left(Y_{n+1/2}(k_0 b) + 2bk_0 Y'_{n+1/2}(k_0 b)\right) - Y_{n+1/2}(k_0 a) \cdot \left(J_{n+1/2}(k_0 b) + 2bk_0 J'_{n+1/2}(k_0 b)\right)\right\} = \left\{k\epsilon_0 J_{n+1/2}(k_0 a)J'_{n+1/2}(ka) - k_0\epsilon J_{n+1/2}(ka)J'_{n+1/2}(k_0 a)\right\} \cdot \left\{Y_{n+1/2}(k_0 b) - J_{n+1/2}(k_0 b) + 2bk_0\left(Y'_{n+1/2}(k_0 b) - J'_{n+1/2}(k_0 b)\right)\right\} \qquad (8)$$

$J'_{n+1/2}$ and $Y'_{n+1/2}$ are the first derived functions ($/k_0 r$ or $/kr$) of $J_{n+1/2}$ and $Y_{n+1/2}$.

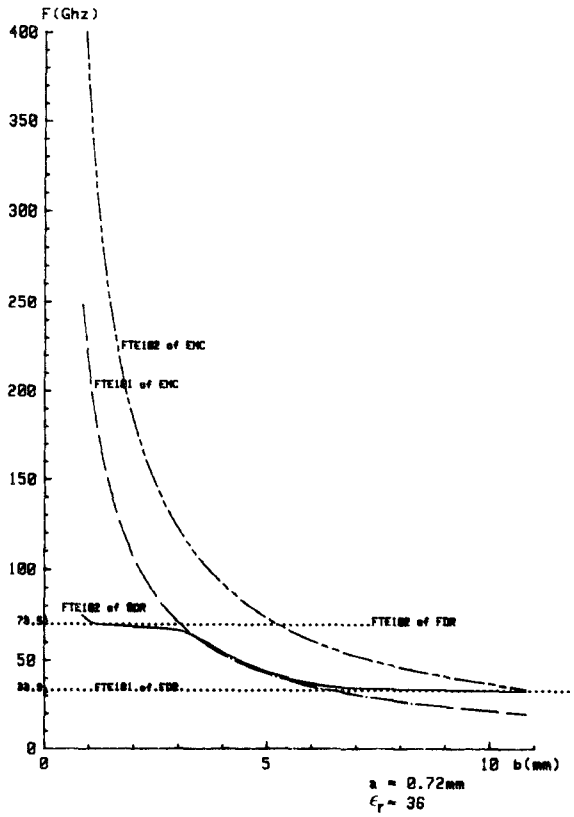

Fig. 4. Resonant frequency variations of the shielded dielectric resonator (SDR) for TE_{102} mode.

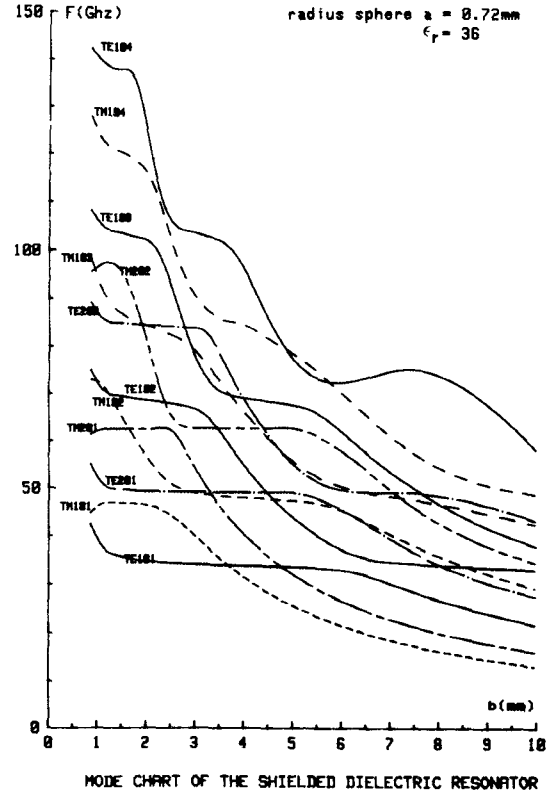

Fig. 6. Mode chart of the first TE_{101}, TE_{201}, TM_{101}, and TM_{201} modes of the SDR.

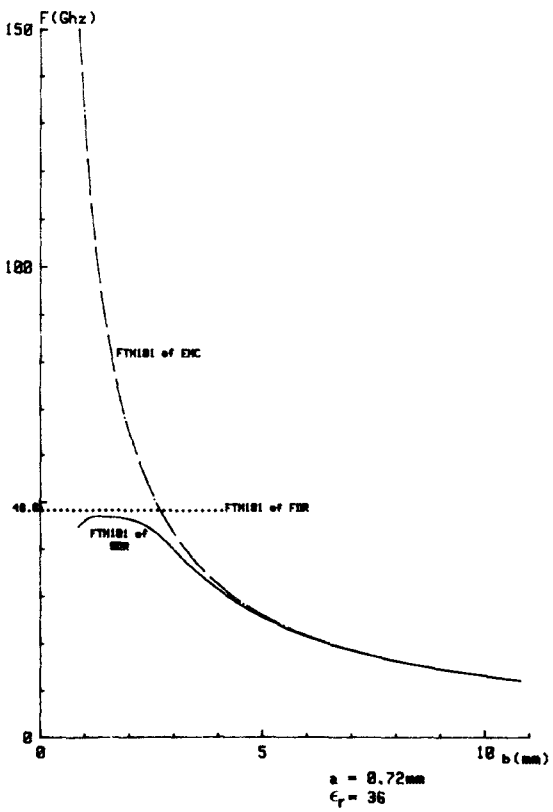

Fig. 5. Resonant frequency variations of the shielded dielectric resonator (SDR) for TM_{101} mode.

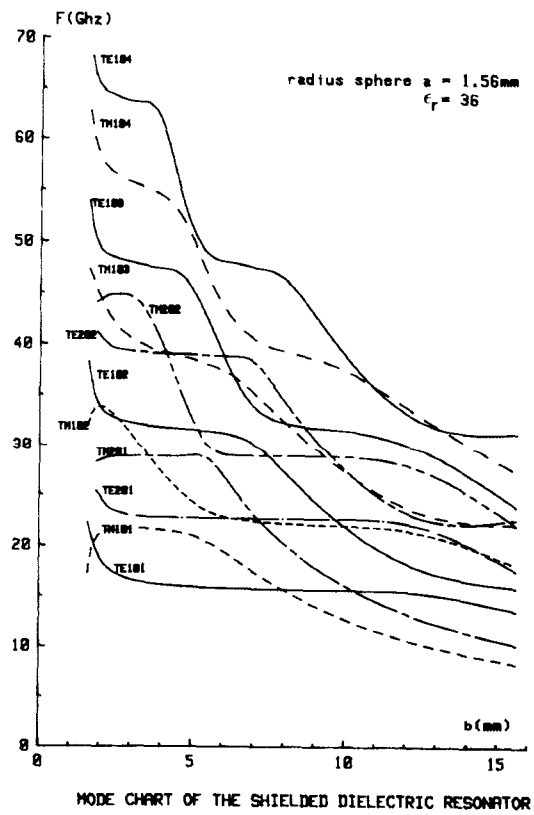

Fig. 7. Mode chart of the first TE_{101}, TE_{201}, TM_{101}, and TM_{201} modes of the SDR.

We solve these equations numerically using a HP9000 computer. The variations of the frequencies as a function of the radius b for $n=1$ and $m=0$ has been drawn in Figs. 3–7.

Let us consider the results for $a=0.72$ mm. For TE_{101} mode, we note that the frequency's plateau ($1<b<6$) corresponds to the resonant frequency of the free sphere, then the frequency variation ($b>6$) follows the variation of the metallic cavity's frequency of the corresponding mode, in which the dielectric resonator is only a small perturbation of this metallic cavity.

This type of variation also can be observed for TM_{101} mode ($1<b<2.5$ & $b>2.5$). For modes that have large i variation (for example $TE_{102}, TE_{103}\cdots$), we see several plateaus that correspond to TE_{104}, i.e.,

the first plateau ($1<b<1.8$)	to	resonant frequency of the free sphere on the TE_{104} mode
the second plateau ($2.5<b<.35$)	to	resonant frequency of the free sphere on the TE_{103} mode
the third plateau ($5<b<7$)	to	resonant frequency of the free sphere on the TE_{102} mode.

Each plateau is followed by the frequency decrease like TE_{101}, TE_{102}, TE_{103}, respectively, modes of the empty cavities corresponding. We can remark that the first plateau (before the convergence to the variation of the TE_{101} of the empty cavity) reduces as the order of the mode increases:

for TE_{101} there is the plateau for $1<b<6$
for TE_{102} there is the plateau for $1<b<3$
for TE_{103} there is the plateau for $1<b<2$
for TE_{104} there is the plateau for $1<b<1.8$.

Finally, a mode chart of the first TE_{101}, TM_{101}, TE_{201}, TM_{201} modes of a shielded dielectric resonator is given.

C. Energy, Losses, and Quality Factor

Energy: The energy $\overline{W}$ stored in the dielectric shielded sphere is defined as:

$$\overline{W}=\frac{1}{2}\epsilon\iiint_v \vec{E}\cdot\vec{E}^*\,dv=\frac{1}{2}\mu\iiint_v \vec{H}\cdot\vec{H}^*\,dv \tag{9}$$

so $\overline{W}$ is the sum of the energy $\overline{W}_1$, stored inside the dielectric sphere (for $r\leqslant a$) and the energy $\overline{W}_2$, stored between the dielectric resonator and the metallic surface ($a\leqslant r\leqslant b$).

Following the mode that we study, $\overline{W}_1$ and $\overline{W}_2$ can be expressed by using either E- or H-field components. For TE_{101} mode we use E, and for TM_{101} mode we use H. In the first case, for example, $\overline{W}_1$ and $\overline{W}_2$ satisfy (10) and (11), respectively

$$\overline{W}_1=\frac{1}{2}\epsilon_0\epsilon_r\int_0^{2\pi}\int_0^{\pi}\int_0^{a}\vec{E}\cdot\vec{E}^*r^2\sin\theta\,dr\,d\theta\,d\phi \tag{10}$$

$$\overline{W}_2=\frac{1}{2}\epsilon_0\int_0^{2\pi}\int_0^{\pi}\int_a^{b}\vec{E}\cdot\vec{E}^*r^2\sin\theta\,dr\,d\theta\,d\phi. \tag{11}$$

We have calculated $\overline{W}_1$ and $\overline{W}_2$ for TE_{101} and TM_{101} modes (i.e., $n=1$ and $m=0$)

TE_{101} Mode

$$J_{n+1/2}(x)=\sqrt{\frac{2x}{\pi}}\,j_n(x)$$

$$Y_{n+1/2}(x)=\sqrt{\frac{2x}{\pi}}\,y_n(x). \tag{12}$$

Applying the relations (12) between the Bessel functions of fractional order $J_{n+1/2}$ and $Y_{n+1/2}$ and the spherical Bessel functions j_n, y_n we obtain (13), (14)

$$\overline{W}_1=\frac{4}{3}A^2\epsilon_0\epsilon_r(2\pi f_0)^2\mu_0^2a^3\cdot\left(j_1^2(ka)-j_0(ka)\,j_2(ka)\right) \tag{13}$$

$$\overline{W}_2=\frac{4}{3}A^2\epsilon_0\mu_0^2(2\pi f_0)^2\cdot\left(B_1^2I_1+C_1^2I_2+B_1C_1I_3\right) \tag{14}$$

with

$$B_1=\frac{-j_1(ka)\,y_1(k_0b)}{j_1(k_0b)\,y_1(k_0a)-j_1(k_0a)\,y_1(k_0b)};$$

$$C_1=\frac{j_1(ka)\,j_1(k_0b)}{j_1(k_0b)\,y_1(k_0a)-j_1(k_0a)\,y_1(k_0b)}$$

$$I_1=r^3\left(j_1^2(k_0r)-j_0(k_0r)\,j_2(k_0r)\right)\Big]_a^b;$$

$$I_2=r^3\left(y_1^2(k_0r)-y_0(k_0r)\,y_2(k_0r)\right)\Big]_a^b$$

$$I_3=r^3\left(2j_1(k_0r)\,y_1(k_0r)-j_0(k_0r)\,y_2(k_0r)-j_2(k_0r)\,y_0(k_0r)\right)\Big]_a^b \tag{15}$$

TM_{101} mode

$$W_1'=\tfrac{4}{3}A^2\mu_0(2\pi f_0)^2\epsilon_0^2\epsilon_r^2a^3\cdot\left(j_1^2(ka)-j_0(ka)\,j_2(ka)\right) \tag{16}$$

$$W_2'=\tfrac{4}{3}A^2\mu_0(2\pi f_0)^2\epsilon_0^2\left(B_2^2I_1+C_2^2I_2+B_2C_2I_3\right) \tag{17}$$

$$B_2=\frac{-\epsilon_r j_1(ka)\left(y_1(k_0b)+bk_0y_1'(k_0b)\right)}{D};$$

$$C_2=\frac{\epsilon_r j_1(ka)\left(j_1(k_0b)+bk_0j_1'(k_0b)\right)}{D}$$

$$D=y_1(k_0a)\left(j_1(k_0b)+bk_0j_1'(k_0b)\right)-j_1(k_0a)\left(y_1(k_0b)+bk_0y_1'(k_0b)\right) \tag{18}$$

j_n' and y_n' are the first derived functions of j_n and y_n.

Losses: The power losses $\overline{P}$ of the system are defined as: $\overline{P}=\overline{P}_m+\overline{P}_d$ where $\overline{P}_m$ are the metallic losses in $r=b$

$$\overline{P}_m=\frac{1}{2}R_s\iint_{\text{metallic surface S}}\left(\vec{H}\cdot\vec{H}^*\right)_{r=b}dS \tag{19}$$

and $\overline{P}_d$ the dielectric losses

$$\overline{P}_d=\frac{1}{2}\sigma_d\iiint_{v\ \text{dielectric sphere volume}}\vec{E}\cdot\vec{E}^*\,dv \tag{20}$$

with

Rs the surface resistivity $=1/\sigma\delta$
σ metallic conductivity
δ skin depth $=\sqrt{2/\omega\mu_0\sigma}$

so

$$Rs=\sqrt{2\pi f_0\mu_0/2\sigma}$$

σ_d is dielectric conductivity $=(2\pi f_0)\epsilon_0\epsilon_r tg\delta$ ($tg\delta$ loss tangent of the material).

As for the energy, we have calculated $\overline{P}$ for TE_{101} and TM_{101} modes

TE_{101} mode

$$\overline{P}_m = \frac{8}{3}A^2\sqrt{\frac{2\pi f_0\mu_0}{2\sigma}}\, b^2k_0^2 \cdot\left(B_1 j_1'(k_0b) + C_1 y_1'(k_0b)\right)^2 \tag{21}$$

$$\overline{P}_d = \frac{1}{2}(2\pi f_0)\epsilon_0\epsilon_r tg\delta\frac{W_1}{\frac{1}{2}\epsilon_0\epsilon_r} = 2\pi f_0 tg\delta W_1 \tag{22}$$

TM_{10l} Mode

$$\overline{P}_m = \frac{8}{3}A^2\sqrt{\frac{2\pi f_0\mu_0}{2\sigma}}\, b^2(2\pi f_0)^2\epsilon_0^2 \cdot\left(B_2 j_1(k_0b) + C_2 y_1(k_0b)\right)^2 \tag{23}$$

$$\overline{P}_d = 2\pi f_0 tg\delta W_1'. \tag{24}$$

Quality Factor Q:

$$Q = 2\pi f_0\frac{\text{energy stored}}{\text{losses}} = 2\pi f_0\frac{\overline{W}}{\overline{P}} \tag{25}$$

i.e.,

$$Q = 2\pi f_0\frac{\overline{W}}{\overline{P}_m + \overline{P}_d}$$

$$\frac{1}{Q} = \frac{\overline{P}_m + \overline{P}_d}{2\pi f_0\cdot\overline{W}}. \tag{26}$$

This Q relation can be written as follows

$$\frac{1}{Q} = \frac{\overline{P}_m}{2\pi f_0\overline{W}} + \frac{\overline{P}_d}{2\pi f_0\overline{W}} = \frac{1}{Q_m} + \frac{1}{Q_d} \tag{27}$$

where Q_m is called the metallic quality factor and Q_d the dielectric one. For the TE_{101} and TM_{101} modes, this Q factor satisfies

TE_{101} mode

$$\frac{1}{Q_m} = \overline{P}_m/\left(2\pi f_0(\overline{W}_1 + \overline{W}_2)\right)$$

$$\frac{1}{Q_d} = tg\delta\overline{W}_1/(\overline{W}_1 + \overline{W}_2)$$

$$Q = \frac{2\pi f_0(\overline{W}_1 + \overline{W}_2)}{\overline{P}_m + 2\pi f_0 tg\delta\overline{W}_1}. \tag{28}$$

TM_{10l} mode

As previously mentioned, we have

$$Q = \frac{2\pi f_0(\overline{W}_1' + \overline{W}_2')}{\overline{P}_m + 2\pi f_0 tg\delta\overline{W}_1'}. \tag{29}$$

III. Results

These Q factors have been computed and the variations as a function of radius b have been drawn in Figs. 8–11.

For TE_{101} and TM_{101}, respectively, the Q plateau (corresponding to the frequencies' plateau) corresponds to the inverse of the loss tangent of the dielectric material. This plateau for TE_{101} ($1 < b < 6$) corresponds to the value $H_\theta = 0$ (Fig 9). Then the increase of Q values (corresponding to the decrease of the frequencies) converges to the Q variation of the metallic cavity. This Q variation is of the same type for the TM_{101} mode.

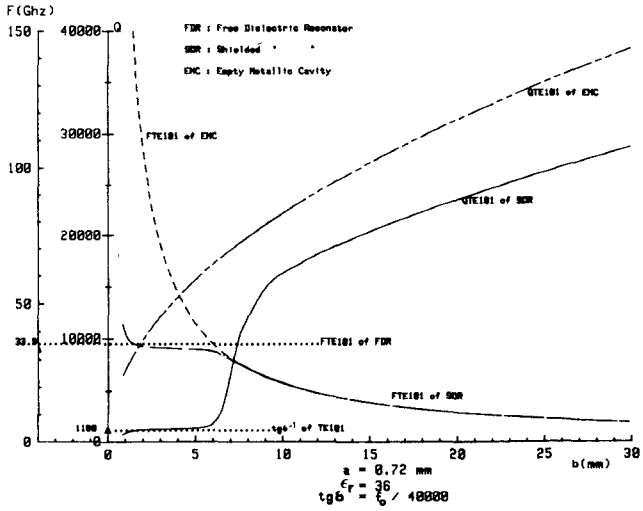

Fig. 8. Quality factor variations of the SDR for TE_{101} mode.

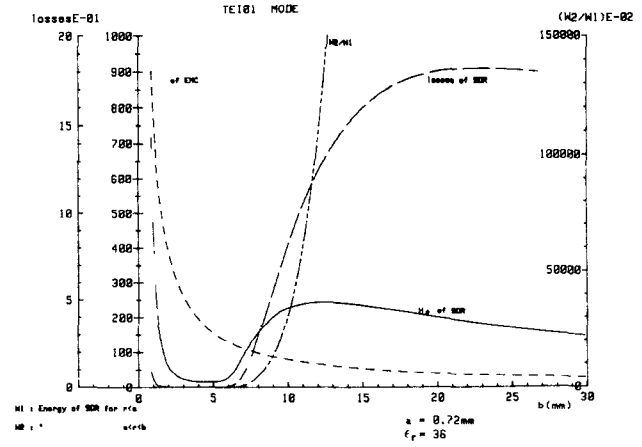

Fig. 9. Energy, losses, and magnetic-field component H_θ for TE_{101} mode.

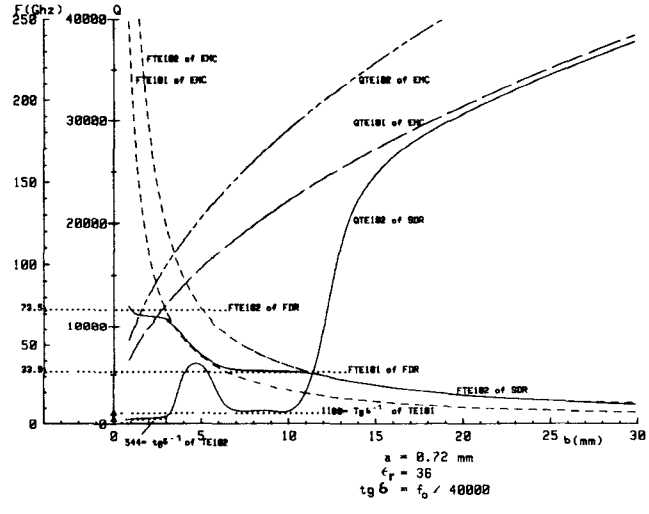

Fig. 10. Quality factor variations of the SDR for TE_{102} mode.

For modes having large i variation, we note several Q plateaus. For TE_{102} for example:

The first Q plateau ($1 < b < 3$) corresponds to the inverse of the loss tangent of the dielectric material on TE_{102} mode (i.e., like for frequencies).

The variation following (i.e., increase and decrease) corresponds to the variation of the Q of the metallic cavity on

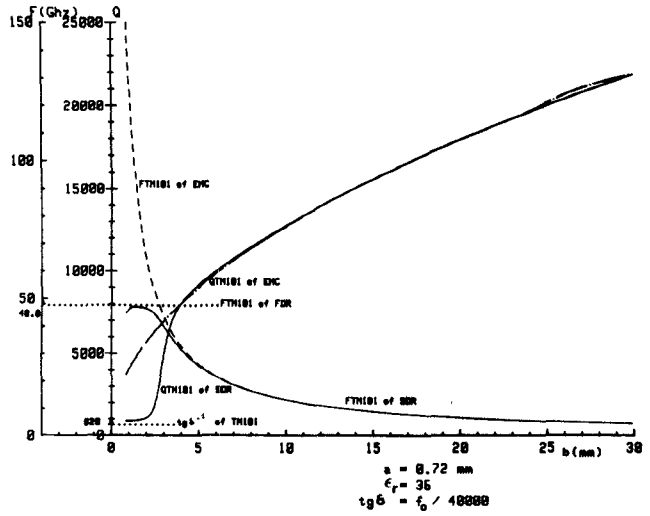

Fig. 11. Quality factor variations of the SDR for TM_{101} mode.

the TE_{101} mode (effectively, here, the resonant frequency of the shielded dielectric resonator on the TE_{102} mode follows the variation of the resonant frequency of metallic cavity on the TE_{101} mode).

The second Q plateau ($7 < b < 10$) corresponds to the inverse of the loss tangent of the dielectric material on the TE_{101} mode.

The last increase converges to the Q values of the metallic cavity on the TE_{102} mode (the frequency follows here, the one of metallic cavity on TE_{101} mode).

ACKNOWLEDGMENT

We thank D. Kajfez for his valuable comments.

REFERENCES

[1] J. Broc, "On the characteristics of electromagnetic resonant cavities formed by two concentric spheres," *C.R. Acad. Sei* (Paris), vol. 230, pp. 198–200, 1950.
[2] H. Y. Yee, "An investigation of microwave dielectric resonators," M. L. Rep. No. 1065, Stanford Univ., July 1963.
[3] M. Gastine, "Résonances électromagnétiques d'échantillons diélectriques," Thése de docteur 3^m cycle, Faculté des Sciences d'Orsay, 1967.
[4] P. Affolter, Eliasson, "Electromagnetic resonances and Q-factor of lossy dielectric spheres," *IEEE*, no. 9, Sept. 1973.
[5] P. Affolter, A. Käch, "Resonance frequencies of a dielectric sphere contained within a concentric shield," *Arch. Elektr. Übertragungstechn.*, (AEÜ), vol. 27, no. 10, pp. 423–432, (in German).
[6] I. Wolff, H. Hofmann, "The three-layer sphere resonator," *Frequenz*, vol. 27, no. 5, pp. 110–119, 1973, (in German).
[7] I. Wolff, N. Schwab, "Measurement of the dielectric constant of anisotropic dielectric materials, using the degenerated modes of a spherical cavity, in *Proc. 10th Euro. Microwave Conf.*, (Warszaw) 1980, pp. 241–245.
[8] NTK: Technical Ceramics Division, NGK spark plugs-Catalog

Accurate Approach for Computing Quasi-Static Parameters of Symmetrical Broadside-Coupled Microstrips in Multilayered Anisotropic Dielectrics

MANUEL HORNO, MEMBER, IEEE, AND FRANCISCO MEDINA

Abstract **— In this paper, we present a method for calculating the propagation parameters of shielded broadside- and broadside edge-coupled microstrip transmission lines. Conductor strips are assumed to be embedded in a multilayered isotropic and/or anisotropic medium. This method provides accurate expressions for computing upper and lower bounds for the true values of mode capacitances. The effects of side wall-shielding and anisotropy of the material are investigated. Some particular multilayered structures are analyzed, which could be applied to the design of directional couplers and filters.**

Manuscript received August 8, 1985; revised January 23, 1986. This work was supported in part by the Comisión Asesora de Investigación Científica y Técnica, Spain.

The authors are with the Departamento de Electricidad y Electronica, Facultad de Fisica, Universidad de Sevilla, 41012, Seville, Spain.

IEEE Log Number 8607967.

I. INTRODUCTION

As is well known, coupled lines are extensively used as building blocks for a great variety of microwave circuit components for communication systems [1]–[3]. The electrical response of coupled line systems has been studied using the ABCD or impedance matrix formulation [4], [5], and these techniques require prior knowledge of the mode characteristic impedances and phase velocities of the structure to be used. When weak coupling must be achieved, edge-coupled strips on a dielectric substrate are widely used. This configuration yields small deviations from equal mode-phase velocities, but these can be suppressed by using adequate techniques [6], [7]. However, if a strong coupling is needed, broadside-coupled configurations are more adequate. If the strips are embedded in an inhomogeneous and/or anisotropic dielectric medium, deviations from equality of phase velocities appear. In fact, large phase velocity ratios can be achieved with broadside-coupled structures, which is useful for the design of single section components with complex electrical responses [8]. Nevertheless, if equal mode-phase velocities are required, matching can be achieved if we use multidielectric iso/anisotropic configurations.

Broadside-coupled and broadside edge-coupled structures have been studied by several authors using different methods [8]–[15]. The purpose of this paper is to present a unified formulation to analyze these configurations, in a multilayered iso/anisotropic medium. The multiple boundaries problem is treated by using a variational method in the spectral domain. The application of this method provides two numerically efficient algorithms that yield upper and lower bounds for the exact values of the mode capacitances for this type of transmission lines. We have applied the method to several particular cases, and also reported the influence of the side walls and anisotropy.

II. ANALYSIS

The cross sections of the structures that are the object of this study are represented in Fig. 1. For both configurations we will assume perfect conductors and lossless dielectric layers. We will also assume strips with valueless thickness. The electrical permittivity of the i-th dielectric layer is given by the following diagonal tensor:

$$\bar{\epsilon}_i = \epsilon_o \begin{bmatrix} \epsilon_x^i & 0 \\ 0 & \epsilon_y^i \end{bmatrix}, \qquad i = 1, \cdots, N. \tag{1}$$

Although the inhomogeneous nature of the dielectric medium precludes pure TEM-mode propagation, one can use the quasi-TEM approximation as long as the cross-sectional dimensions are much smaller than the wavelength. In this case, structures in Fig. 1(a) and (b) can support two and four orthogonal modes of propagation, respectively. By determining each mode capacitance, we can in turn discover the electrical behavior of the coupled transmission line. To evaluate the mode capacitances, one can simplify the problem by taking into account the symmetry of the structure. In fact, we only need analyze one quadrant of the cross section shown in Fig. 1(a) or (b) (the upper right